Energy 232 (2021) 121055

Contents lists available at ScienceDirect

Energy

journal homepage: www.elsevier.com/locate/energy

Osmotic engine converting energy from salinity difference to a hydraulic accumulator by utilizing polyelectrolyte hydrogels

Tri Quang Bui [a, b], Ole-Petter Magnussen [a], Vinh Duy Cao [a], Wei Wang [b], Anna-Lena Kjøniksen [a, *], Olav Aaker [a, **]

[a] Faculty of Engineering, Østfold University College, P.O. Box 700, 1757, Halden, Norway
[b] Department of Chemistry & Center for Pharmacy, University of Bergen, P.O. Box 7803, 5020, Bergen, Norway

ARTICLE INFO

Article history:
Received 21 September 2020
Received in revised form
14 April 2021
Accepted 24 May 2021
Available online 25 May 2021

Keywords:
Osmotic engine
Salinity gradient
Energy transmission
Hydrogel

ABSTRACT

Efficient harvesting of the mixing energy from the salinity gradient between sea and river water remains a challenge. Recently, utilization of the swelling/shrinking properties of hydrogels has been explored as a new means for extracting this energy. However, former investigations are mainly limited to examining the performance of the hydrogels when lifting applied weights, and calculating the energy that could potentially be extracted. In this study, we demonstrate a novel osmotic engine with a mechanical energy transmission prototype, which can convert and store the green mixing energy in a form that can be utilized to perform mechanical work. The osmotic engine includes a cylinder containing the hydrogel, an oil-hydraulic cylinder and a hydraulic accumulator. The lifting energy from the hydrogel is transferred to the oil-hydraulic cylinder through a lever, which acts as a pump and accumulate the hydraulic oil under high pressure in the hydraulic accumulator. The system was tested with a hydrogel of poly(acrylic acid) semi-interpenetrated with poly(4-styrenessulfonic acid-*co*-maleic acid) sodium. This hydrogel produced up to 36 J per shrinking/swelling cycle, and exhibited an efficiency of 0.53% at optimum conditions.

1. Introduction

With a need of reducing CO_2 emissions and replacing fossil fuel with more sustainable energy sources, great efforts are aimed at capturing and utilizing renewable energy such as solar, wind, geothermal, or ocean. The difference in salinity of two liquids produce entropic energy upon mixing. Chemical energy from the salinity gradient between seawater and freshwater is therefore a substantial potential power source [1]. The mixing energy when river water flows into the ocean is estimated to be 2.2 kJ per liter of fresh water [2]. Although concepts such as exploiting the differences in vapor pressure between salt and freshwater has been suggested [3,4], the currently most reliable techniques to harvest energy from mixing seawater with river water utilize membranes [2]. Pressure-retarded osmosis (PRO) [5–8], reverse electro-dialysis (RED) [9–11], and capacitive mixing (CapMix) [12–15] have been explored to extract salinity gradient energy.

Recently, Zhu et al. proposed a new and interesting method utilizing hydrogels to convert mixing energy into mechanical energy [16]. The method is based on the different swelling of hydrogels in seawater and freshwater. Charged hydrogels swell in freshwater, since the charges attached to the polymer chains repel each other. In saltwater, the large amounts of free ions screen out the electrostatic repulsive forces, and the hydrogels contracts to a smaller volume. In addition, for most polymer systems freshwater is a better solvent than saltwater, causing the polymer chains (and the hydrogels) to contract in saltwater even for neural polymers [17]. The swelling/deswelling of the hydrogel can be utilized to lift a piston in an osmotic engine in swelling-shrinking cycles [18–21]. Previous studies have shown recovered energies of 0.34–102 J per gram dried polymer utilized [21]. It should however be noted that this technology is still in its infancy, and there are a range of parameters that need to be improved and optimized to achieve a high energy output. The advantage of this technology is the low cost of the hydrogels, and that it is easier to maintain, replace, and reuse the hydrogels than for membrane-based technologies. However, a great drawback of this technique is that the current systems have cycles that takes a very long time. In addition, there is a lack of osmotic engines that convert the energy into a convenient useable

* Corresponding author.
** Corresponding author.
E-mail address: anna.l.kjoniksen@hiof.no (A.-L. Kjøniksen).

https://doi.org/10.1016/j.energy.2021.121055

form.

Hydraulic systems are often applied for energy transmission. They can be used to convert the energy from an electric motor to a large force applied at low speed [22], or to produce electricity from wave energy [23,24]. Energy regeneration and conversion technology based on a hydraulic transmission systems have applications in construction machinery, hydraulic vehicles, and regenerative suspensions [25]. The hydraulic transmission system transforms the waste energy (gravitational potential energy in a hydraulic excavator [26], braking energy when vehicles deaccelerate [27,28], and vibration kinetic energy in the suspension system of a vehicle [29,30]) into energy stored in a battery, supercapacitor, or accumulator. Hydraulic transmission systems based on wave energy uses a float to capture wave energy. The wave causes the float to move vertically up and down with respect to the hydraulic cylinder. The motion of the buoy is converted into electric energy [23].

While previous works have utilized smaller systems with small hydrogel volumes, this work presents the development of a scaled-up osmotic engine, which includes a novel mechanical energy transmission prototype. The osmotic engine extracts the entropic mixing energy from two aqueous solutions of different salinity by utilizing the swelling/deswelling of hydrogels. The energy is stored in a hydraulic accumulator.

2. Methods

2.1. Operational principle of the osmotic engine

As shown in Fig. 1, the osmotic engine consists of the following components: (a) a large cylinder with a diameter of 240 mm, which contains the hydrogel, (b) a weight which increases the downward motion during the shrinking process, (c) a lever which connects the hydrogel cylinder to (d) an oil hydraulic cylinder. When the hydrogel expands the hydraulic oil piston is pressed downward, thereby pumping the oil into (f) the accumulator. The accumulator has a working pressure that should ideally be constant, but which will increase slightly as the accumulator is filled with oil. Pressurized nitrogen makes the accumulator pressure. When starting the system, the accumulator can be partially filled with oil by a hydraulic pump. The energy stored by the hydraulic oil at high pressure in the accumulator can be utilized for further applications, such as rotating a hydraulic motor to produce electricity.

The freshwater and saltwater were pumped at a rate of 100 mL/min and 40 mL/min, respectively, into the hydrogel cylinder from the holes in the bottom of the cylinder (Fig. 2). The piston on top of the hydrogel has holes through which excess water can escape. The excess water was siphoned off the cylinder from the top. A weight of 10 kg was placed on the top of the piston rod in order to push the piston down during the shrinking of the hydrogel. The piston is connected to the hydraulic oil cylinder by a lever with an adjustable fulcrum, to maximize the energy extracted from the hydrogel expansion. The 25 mm in diameter hydraulic cylinder converts the linear motion into fluid power. To maximize the fluid displacement in the hydraulic cylinder, the perpendicular distance to the pivot is closer to the hydrogel cylinder (20 cm) than to the hydraulic cylinder (22 cm) (Fig. 2). The hydraulic accumulator stores fluids under high pressure. The pressure in the air bladder of the hydraulic accumulator increase as larger amounts of fluid flow inward. The fluid pressure in both the hydraulic cylinder and the accumulator was detected by a pressure sensor and a gauge. An oil pump was utilized to produce the initial pressure for the accumulator, and functions as a low-pressure fluid supply to replace the oil that is pressed into the accumulator.

The dried hydrogel (50 g) was swelled to equilibrium in distilled water, before it was inserted in the cylinder. The operational principle of the motor is shown in Fig. 2. In the beginning, valve 1 was opened and valve 2 closed. The oil pump was used to raise the pressure of the system until it was equal to the pressure of compressed nitrogen in the accumulator. Then valve 1 was closed to avoid leakage back to the oil pump. A seawater-like solution (35 g/L NaCl) was pumped through the hydrogel cylinder, which cause the hydrogel to contract and the piston above the hydrogel to move down. This lifts the piston in the hydraulic oil cylinder, allowing the low-pressure oil to fill into the lower part of the hydraulic oil cylinder (valve 3 opened, valve 2 closed). At the same time, the oil in the upper part of the hydraulic oil cylinder is driven back to the oil pump. When the hydrogel is close to its minimum height, the piston in the hydraulic oil cylinder is in position 0 (Fig. 2). At this point, the system switches to pumping freshwater through the hydrogel cylinder. After this, the hydrogel keeps shrinking during the time it takes to flush the saltwater out of the system. Since closing valve 3 during shrinking of the hydrogel might give rise to air in the hydraulic cylinder, valve 3 was kept open for an additional 10–20 min before it was closed.

When freshwater has displaced the saltwater, the hydrogel swells. The hydrogel pushes the piston above it upwards, causing

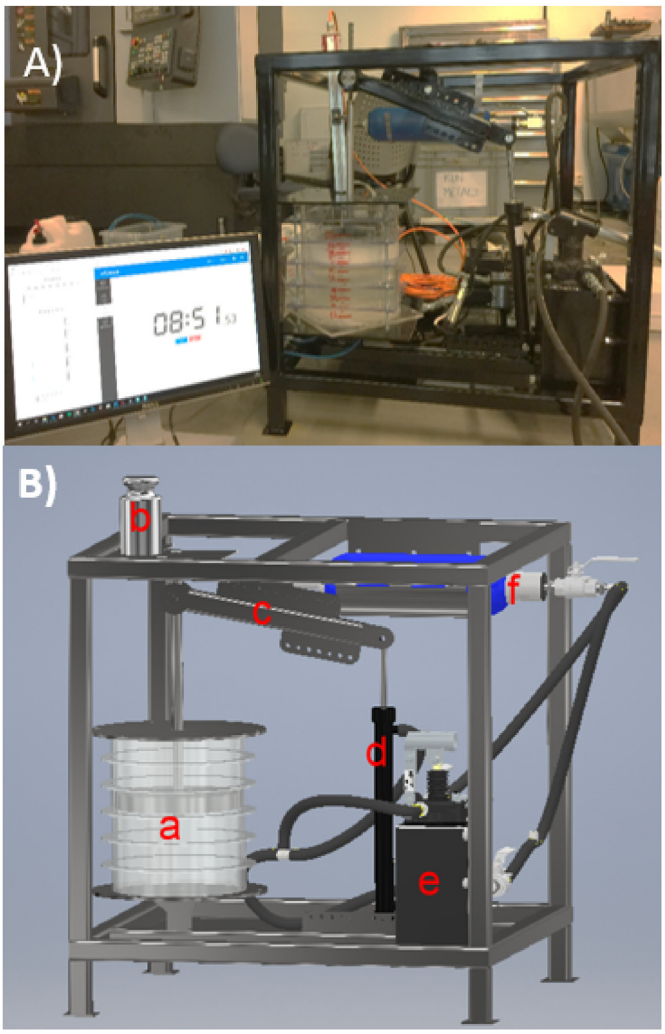

Fig. 1. A) Picture of the osmotic engine, and B) sketch of the components of the osmotic engine (a) cylinder which contains the hydrogel; (b) weight; (c) lever; (d) hydraulic oil cylinder; (e) hydraulic oil pump; (f) accumulator.

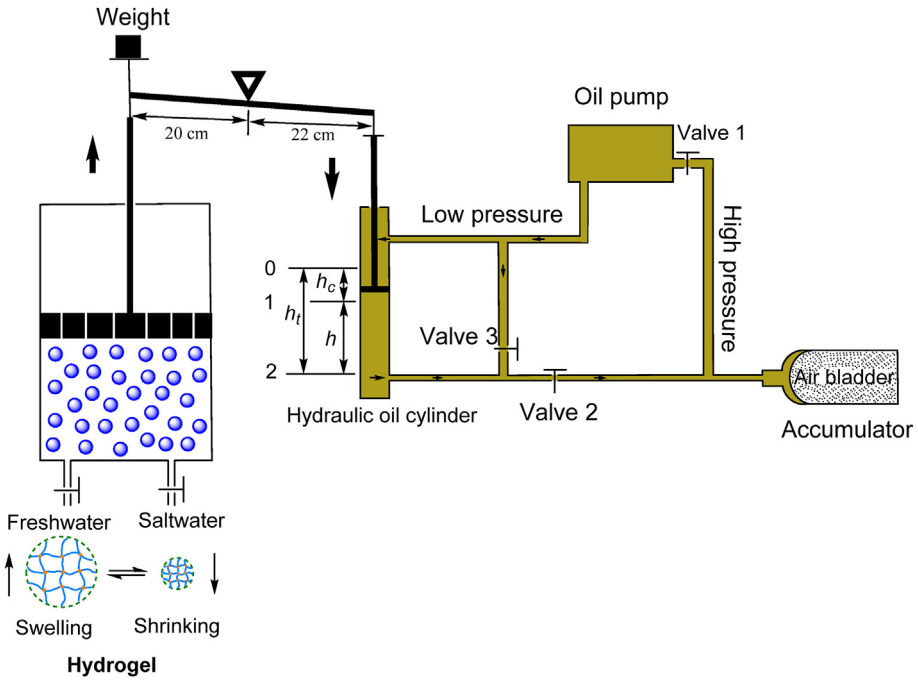

Fig. 2. Operation principle of the osmotic engine.

the piston of the hydraulic cylinder to move down. This increases the pressure of the hydraulic oil. Valve 2 is opened when the pressure in the lower part in the hydraulic cylinder becomes higher than the pressure in the accumulator. At this point, the hydraulic piston has reached position 1 (Fig. 2) with a compressed displacement height of h_c. After valve 2 is opened, hydraulic oil is pressed into the accumulator by further expansion of the hydrogel. At the maximum expansion of the hydrogel, the hydraulic piston is at position 2 (Fig. 2), with a total displacement height of h_t. The distance the hydraulic piston moves from position 1 to position 2 is the stored displacement height (h). At this point, valve 2 was closed and valve 3 was opened for the next cycle. The total cycle time was adjusted according to the swelling ratio and lifting capacity of the hydrogel, thereby ensuring that the displacement height (h_t) is higher than the compressed displacement height (h_c).

2.2. Produced energy and energy efficiency

The work (W_g) the hydrogel conducts on the hydraulic accumulator in form of compressing the nitrogen gas to a higher pressure can be expressed as:

$$W_g = -\int_{V_s}^{V_e} p dV \tag{1}$$

where p is the pressure in the accumulator, and V_s and V_e are the volume of the nitrogen gas in the accumulator at the start and end of the swelling cycle, respectively. Assuming the nitrogen behaves as an ideal gas, we can use $pV = nRT$, where n is the amount of gas in moles, T the absolute temperature (298 K), and R (8.314 $\mathrm{Jmol^{-1}K^{-1}}$) the gas constant. Substituting into eq. (1) and performing the integration gives:

$$W_g = nRT \ln\frac{V_s}{V_e} \tag{2}$$

The volume change ΔV during the cycle is given by $\Delta V = V_s\text{-}V_e$. Assuming no gas leakage and a constant temperature: $p_s V_s = p_e V_e$, where p_s and p_e are the pressure in the accumulator at the start and end of the swelling cycle, respectively. Accordingly, $V_s = \frac{p_e \Delta V}{p_e - p_s}$ and $V_e = \frac{p_s \Delta V}{p_e - p_s}$, which gives $\frac{V_s}{V_e} = \frac{p_e}{p_s}$ and $nRT = \frac{p_s p_e \Delta V}{p_e - p_s}$. The change in volume of the gas equals the volume of oil pressed into the accumulator by the hydraulic oil cylinder: $\Delta V = \pi r^2 h$, where r is the radius of the hydraulic oil cylinder (12.5 mm), and h is the height the piston moves while the oil is pressed into the accumulator (Fig. 2). Substituting into eq.(2) gives the work expressed by easily measured quantities:

$$W_g = \frac{p_s p_e \pi r^2 h}{p_e - p_s} \ln\frac{p_e}{p_s} \tag{3}$$

The power (P) produced during one cycle is:

$$P = \frac{W_g}{\Delta t} \tag{4}$$

where Δt is the time of one cycle.

The mixing energy (E_{mix}) when mixing saltwater with freshwater can be expressed as [16]:

$$E_{mix} = RT \sum_i \left(n_{sw} \ln\frac{\alpha_{i,sw}}{\alpha_{i,mix}} + n_{fw} \ln\frac{\alpha_{i,fw}}{\alpha_{i,mix}} \right) \tag{5}$$

where n_{sw} and n_{fw} the number of mol NaCl in the saltwater and freshwater, respectively. $\alpha_{i,sw}$, $\alpha_{i,fw}$, and $\alpha_{i,mix}$ is the activity of the ionic species i in the saltwater, freshwater, and mixed solution, respectively. Since the freshwater in this case is pure water without NaCl ($n_{fw} = 0$), eq. (5) reduces to:

$$E_{mix} = RTn_{sw} \left(\ln\frac{\alpha_{Cl^- sw}}{\alpha_{Cl^- mix}} + \ln\frac{\alpha_{Na^+ sw}}{\alpha_{Na^+ mix}} \right) \tag{6}$$

The activity can be expressed as [31] $\alpha_i = m_i \gamma_i$, where m_i is the

molality of the ionic species i in the solution, and γ_i is the molality activity coefficient of the ionic species i. The values of γ_i for Na^+ and Cl^- is calculated utilizing the Khoshkbarchi and Vera equation for a 1:1 electrolyte at 25 °C [32,33]:

$$\ln \gamma_i = \frac{-8.766\sqrt{I_x}}{1+9\sqrt{I_x}} + B_i\frac{I_x^{3/2}}{1+9\sqrt{I_x}} + C_i \ln\left(1+9I_x^{2/3}\right) \quad (7)$$

where $B_{Na^+} = 79.62$, $C_{Na^+} = 0.30$, $B_{Cl^-} = 70.57$, $C_{Cl^-} = -0.14$ [32], and $I_x = \frac{m_i}{2m_i+55.55}$.

The work (E_{pump}) performed by the pump that flushes the water through the hydrogel [20] can be expressed as:

$$E_{pump} = p_{g,sh}Q_{sh}\Delta t_{p,sh} + p_{g,sw}Q_{sw}\Delta t_{p,sw} \quad (8)$$

where Q is the flow rate and p_g is the pressure in the gel cylinder, Δt_p is the time the pump is working, and the subscripts sh and sw refers to the shrinking and swelling process, respectively. The total energy supplied into the system (E_{sup}) is:

$$E_{sup} = E_{mix} + E_{pump} \quad (9)$$

The percentage efficiency (η) determines how much of the supplied energy is converted into output energy:

$$\eta = \frac{100W_g}{E_{sup}} \quad (10)$$

For a real-world system, pre-treatment of the supplied water will also contribute to the energy efficiency. It is however currently unclear how much purification is needed to ensure that the osmotic engine will work properly for an extended period of time.

2.3. Hydrogels

Hydrogels of poly(acrylic acid) semi-interpenetrated with poly(4-styrenessulfonic acid-*co*-maleic acid) sodium were prepared by free radical polymerization. Monomer solutions were prepared mixing 60 g acrylic acid monomer (Sigma Andrich) and 24 g poly(4-styrenessulfonic acid-*co*-maleic acid) (Sigma Aldrich) in 468 mL distilled water. The N,N,N′,N′-tetramethylethylenediamine (TEMED, Sigma Aldrich), ammonium persulfate (APS, Sigma Aldrich), and crosslinker N′,N′-methylenebis(acrylamide) (MBA, Sigma Aldrich) was consecutively added to the monomer solutions under stirring. The mixture was purged with nitrogen gas for 10–20 min to remove oxygen, after which the gelation was carried out in an oven at 50 °C. After gelation, the hydrogel was cut into small pieces and immersed in a large quantity of de-ionized water to remove unreacted monomers and catalysts. The dialysis water was changed daily for 5–7 days in order to reach equilibrium swelling for the hydrogels. The hydrogel was dried at 70–80 °C in the oven. Three samples at different crosslinking densities of 1.5% (CD1.5), 3.0% (CD3.0) and 4.0% (CD4.0) were prepared for the further experiments. The swelling ratios of CD1.5; CD3.0; CD4.0 were 201 g/g, 96 g/g, and 44 g/g, respectively.

3. Results and discussion

3.1. Displacement height

The new osmotic engine transforms the lifting energy of the hydrogel into accessible power by accumulating oil in the storage chamber at high pressure. A higher lifting capacity of the hydrogel increases the amount of fluid stored in the accumulator, thereby enhancing the amount of stored energy. Fig. 3 shows the total displacement height of the hydraulic cylinder during one cycle of expansion of the three different hydrogels. To store oil in the accumulator, the oil pressure in the lower part of the hydraulic cylinder should be greater the pressure in the accumulator. In the beginning of the cycle, the piston moves a distance h_c from position 0 to 1 (Fig. 2) to achieve an oil pressure above the accumulator pressure. As can be seen from Fig. 3, the compressed height (h_c) moving from position 0 to position 1 varies from about from 0.5 to 1 cm depending on the hydrogel. There is only a small variation, since the hydraulic oil is an incompressible fluid in which the pressure grows fast with small changes in volume. Fig. 3 also illustrates that it took between 30 min and 3 h before the pressure in the hydraulic cylinder exceeded that in the accumulator (from position 0 to position 1). This is the desalination time of the hydrogel, when saltwater is exchanged with freshwater. Accelerating the time it takes to move from position 1 to position 2 is critical for increasing the power of the osmotic engine. The desalination time might be shortened by enhancing the hydrogel's exposure to water to improve the exchange of saltwater and freshwater within the hydrogel structure, or by utilizing a hydrogel that swells faster. Increasing the rate of and volume of the freshwater and saltwater supplies will enhance the swelling/de-swelling rates of hydrogel and shorten the cycle time. However, this also causes a higher energy demand of the pump supplying the water, thereby decreasing the overall efficiency of the system. This balance should be optimized in further studies. It is important to keep air from entering the hydraulic system, since it is much more compressible than oil. Air mixed in with the oil will therefore significantly reduce the build-up of pressure, thereby rendering the system less efficient.

When the pressure exceeds that in the accumulator, valve 2 is opened and the piston move a distance h from position 1 to 2 (Fig. 2). As the crosslinking density of the hydrogels is raised, the mechanical strength improves while the maximum swelling volume is reduced (crosslinks prevent the hydrogel network from expanding). In addition, at low crosslinking densities the hydrogels swell and shrink faster, since the diffusion of salt/fresh water into the hydrogels is improved [20]. The samples with lower

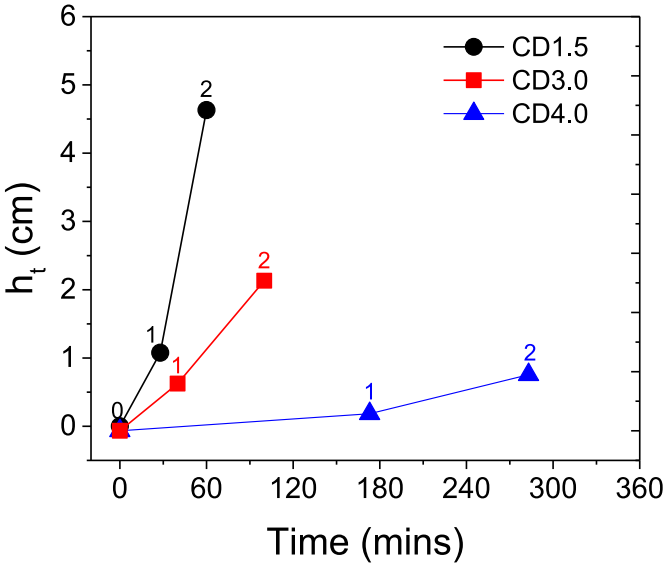

Fig. 3. Total displacement height of the hydraulic cylinder during one cycle. The displacement height from position 0 to position 1 is the compressed height (h_c) and the distance between position 1 and 2 is the stored height (h) at crosslinking densities of 1.5% (CD1.5), 3.0% (CD3.0), and 4.0% (CD4.0).

crosslinking densities therefore expand both faster and to larger volumes (Fig. 3), pushing more oil into the accumulator and thereby improve the power output.

3.2. Cumulative pressure over several cycles

The hydraulic accumulator incorporates a gas bladder in conjunction with a hydraulic fluid. The fluid has little dynamic power-storage qualities, whereas the gas can be compressed into small volumes at high pressure. In the mechanical energy transmission system, the oil flowing from the hydraulic cylinder during each cycle was stored in the accumulator and compressed the air bladder. The increase of fluid volume in the accumulator gives rise to a higher air pressure.

Fig. 4 illustrates that the pressure in the accumulator increases for each cycle as more oil is stored in the accumulator. As explained above, the hydrogel with the lowest crosslinking density of 1.5% (CD1.5) swells more (i.e., h is higher) than the hydrogels with higher crosslinking densities. Accordingly, the cumulative pressure increases much more for each cycle for CD1.5, since a greater amount of fluid is pressed into the accumulator. When the crosslinking density is raised, the hydrogel swells less (h decreases). As a result, the increase of the cumulative pressure is moderate for the crosslinking density of 3.0% (CD3.0), and very little for CD4.0.

3.3. Effect of initial pressure

To optimize the osmotic engine, the initial pressure in the accumulator (supplied by the oil pump), was varied from 12 to 25 bar which corresponds to a pressure on the hydrogel from 0.18 to 0.32 bar. When the initial pressure is raised, the hydrogel with the lowest crosslinking density (CD1.5) provides a higher output energy (Fig. 5a). However, at high initial pressures the output energy decreased again. At higher crosslinking densities, the effect of the initial pressure is more modest, and there was no decline in the power output at initial pressures up to 25 bar. In order to see whether a similar maximum in output energy would be evident at higher pressures, CD3.0 was also measured at an initial pressure of approximately 30 bar. As can be seen from Fig. 5a, the additional measurement confirms that there is an optimum initial pressure, which increases with higher crosslinking densities. Similar maximums in recovered energy has been observed when hydrogels was subjected to swelling/shrinking cycles under increasing external

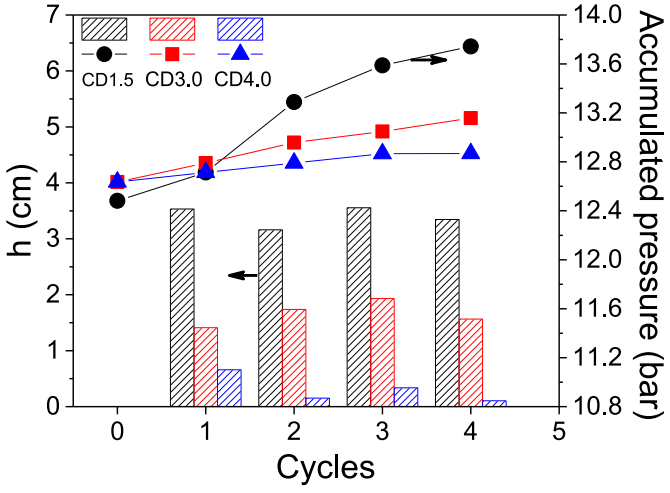

Fig. 4. Displacement height and cumulative pressure of the osmotic engine over 4 cycles at crosslinking densities of 1.5% (CD1.5), 3.0% (CD3.0), and 4.0% (CD4.0).

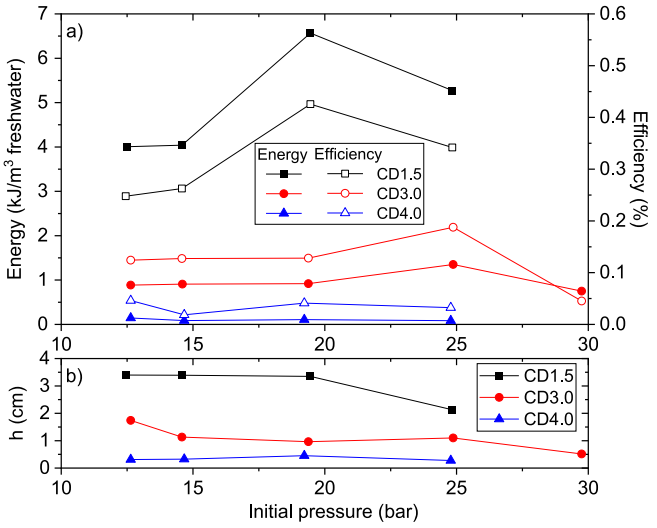

Fig. 5. a) Energy and efficiency generated at different hydrogel crosslinking densities of 1.5% (CD1.5), 3.0% (CD3.0), and 4.0% (CD4.0) as a function of the initially applied pressure. b) Displacement height (h) as a function of the initially applied pressure.

loads [19]. Analogous to Fig. 5a, the maximum was shifted towards higher external loads when the crosslinker concentration was increased [19]. When the initial pressure becomes too high, the swelling of the hydrogels is reduced (Fig. 5b), since they are working against a restricting external force [19]. As can be seen from eq. (3), reducing the displacement height results in a decreased energy production. Accordingly, the observed maxima at medium pressures in Fig. 5a is caused by increased energy production as the hydrogels work against higher external pressures, combined with reduced swelling heights at high pressures reducing the energy production. Interestingly, there is a small upturn at the lowest pressure for the sample with the highest crosslinking density. The reason for this is currently unclear.

The energy efficiencies (Fig. 5a) generally follow the same trends as the generated energies, and reaches 0.53% at optimum conditions. In addition to the produced energy, the energy efficiency is dependent on the amount and concentration of the saltwater (eq. (6)), and for a real-life system it will also depend on the amount of salt in the freshwater supply [19]. In addition, it depends on the energy consumed by the pump that supplies the water (eq.(8)). Accordingly, reducing the amount of water pumped through the system can increase the energy efficiency by reducing the supplied energy, while using too little water will reduce the height difference between the swollen and de-swollen hydrogel and diminish the energy produced by the system. The volumes of supplied water therefore need to be optimized for maximum energy efficiency.

Increasing the crosslinking density of the hydrogel results in a reduction of the performance due to the reduced swelling height (Fig. 5). Accordingly, CD1.5 exhibited the highest energy generation (Fig. 5a), and reached 36 J/cycle (0.13 W/kg hydrogel) at optimum conditions. However, for the highly crosslinked hydrogel (CD4.0), the output energy was only about 4 J/cycle due to the low displacement height (Fig. 5b). In addition, CD4.0 has a very long expansion time (Fig. 3), which results in an extremely low power output (5 mW/kg hydrogel). The optimum crosslinking density (1.5%; CD1.5) is not the same as previously observed for small scale experiments (3%; CD3.0). The discrepancy might be caused by different behavior when the system is scaled up, and by the dissimilarities of the water flow through the hydrogels.

3.4. Repeated cycling

The ability of the hydrogels to continue over several repeated cycles has been demonstrated in small-scale previously [18–20]. Fig. 6a illustrates how the total displacement height (h_t) varies during 10 repeated cycles of CD3.0 utilizing the osmotic engine. Fig. 6b illustrates the accumulative energy production during the 10 cycles. The system produces about 9 J per cycle throughout the 10 cycles. Accordingly, the osmotic engine is capable of operating during multiple repeated cycles, which is promising for further applications.

Although the osmotic engine is capable of delivering the same energies over a number of repeated cycles (Fig. 6b), deviation from linearity is observed at certain conditions. Since the generated energies go through a maximum when the initial pressure is raised (Fig. 5a), and the pressure increases somewhat during each cycle (Fig. 4), the pressure change will eventually cause a deviation from linearity. This is evident for CD1.5 at an initial pressure of 19.5 bar (Fig. 7), where the 4th cycle generates a smaller amount of energy than previous cycles. The lower energy produced during the 4th cycle is related to a significantly lower displacement height (inset in Fig. 7). For the other applied pressures, the energy generation is approximately the same during each of the 4 cycles (Fig. 7), and the displacement heights do not exhibit any obvious reduction from cycle to cycle. It should be noted that when energy is extracted from the hydraulic accumulator (e.g. to produce electricity), this will prevent the build-up of too high pressures. At these conditions, a constant energy production over a high number of cycles is anticipated.

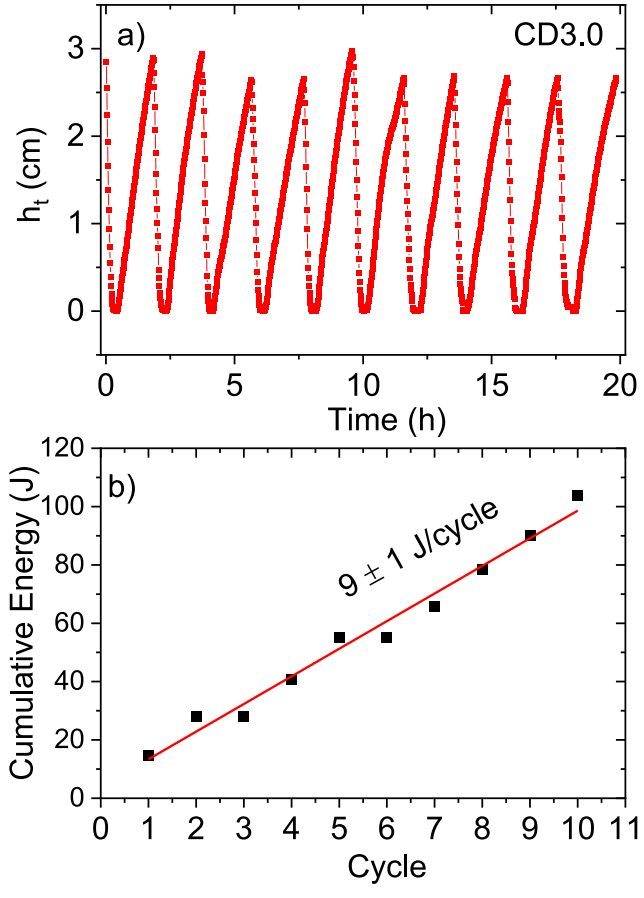

Fig. 6. Repeated hydrogel swelling/shrinking cycles utilizing the osmotic engine with mechanical transmission system. a) The variation of the total displacement height (h_t) during 10 repeated cycles for the system with a crosslinking density of 3% (CD3.0) with an initial pressure of about 12.5 bar. b) The cumulative energy through the 10 repeated cycles. The line is a linear fit to the data.

4. Conclusions

An osmotic engine with a mechanical energy transmission prototype was developed. By utilizing poly(acrylic acid)-based hydrogels that swell in freshwater and shrink in seawater, the osmotic engine could convert the mixing energy of seawater and freshwater into green, accessible power. The energy was stored in a hydraulic accumulator for further applications. The experimental data showed a successful energy accumulation in the accumulator during repeated cycles. The hydrogel with the lowest crosslinking density generated the highest output power, with up to 36 J/cycle (0.13 W/kg hydrogel) at optimum conditions.

The prolonged cycle time of the osmotic engine provides a relatively low power output. However, this is a very new technology with a high potential for future improvement. Enhanced water flow through the hydrogel can decrease the swelling time of the hydrogel, resulting in a much shorter cycling time. However, an optimal system should exhibit a better water exchange into the hydrogel without increasing the utilized amount of water, since the water pump also supplies energy to system. A larger exposed surface area between the hydrogel and the water will probably improve the efficiency of the osmotic engine.

Although the achieved efficiency is low, the prototype exhibits a promising potential for green energy generation.

Credit author statement

Tri Quang Bui: Conceptualization, Methodology, Formal analysis, Investigation, Writing – original draft, Writing – review & editing, Visualization. **Ole-Petter Magnussen**: Methodology, Investigation, Writing – review & editing, Visualization. **Vinh Duy Cao**: Investigation, Writing – review & editing. **Wei Wang**: Writing – review & editing, Supervision. **Anna-Lena Kjøniksen**: Conceptualization, Formal analysis, Writing – review & editing, Visualization, Supervision. **Olav Aaker**: Conceptualization, Methodology, Writing – review & editing, Supervision

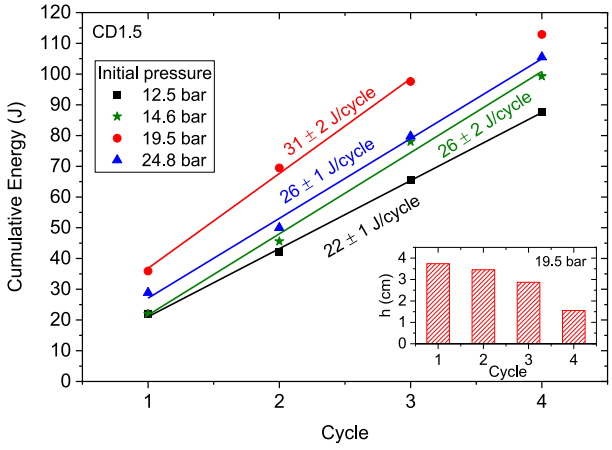

Fig. 7. The cumulative energy over 4 cycles for the hydrogel with at crosslinking density of 1.5% (CD1.5) at different initial pressures. The lines are linear fits to the data. The inset shows the displacement height (h) as a function of the number of cycles at an initial pressure of 19.5 bar.

Declaration of competing interest

The authors declare that they have no known competing financial interests or personal relationships that could have appeared to influence the work reported in this paper.

References

[1] Norman RS. Water salination: a source of energy. Science 1974;186(4161):350–2.
[2] Mantia FL, Pasta M, Deshazer HD, Logan BE, Cui Y. Batteries for efficient energy extraction from a water salinity difference. Nano Lett 2011;11(4):1810–3.
[3] da Rosa AV. Fundamentals of renewable energy processes. London, UNITED STATES: Elsevier Science & Technology, 2005.
[4] Olsson M, Wick GL, Isaacs JD. Salinity gradient power: utilizing vapor pressure differences. Science 1979;206(4417):452–4.
[5] Straub AP, Deshmukh A, Elimelech M. Pressure-retarded osmosis for power generation from salinity gradients: is it viable? Energy Environ Sci 2016;9:31–48.
[6] Logan BE, Elimelech M. Membrane-based processes for sustainable power generation using water. Nature 2012;488(7411):313–9.
[7] Loeb S, Norman RS. Osmotic power plants. Science 1975;189(4203):654–5.
[8] Achilli A, Childress AE. Pressure retarded osmosis: from the vision of Sidney Loeb to the first prototype installation — Review. Desalination 2010;261(3):205–11.
[9] Post JW, Hamalers HVM, Buisman CJN. Energy recovery from controlled mixing salt and fresh water with a reverse electrodialysis system. Environ Sci Technol 2008;42(15):5785–90.
[10] Veerman J, Saakes M, Metz SJ, Harmsen GJ. Reverse electrodialysis: evaluation of suitable electrode systems. J Appl Electrochem 2010;40(8):1461–74.
[11] Pattle RE. Production of electric power by mixing fresh and salt water in the hydroelectric pile. Nature 1954;174:660.
[12] Rica R, Ziano R, Salerno D, Mantegazza F, van Roij R, Brogioli D. Capacitive mixing for harvesting the free energy of solution at different concentrations. Entropy 2013;15(12):1388–407.
[13] Hatzell MC, Raju M, Watson VJ, Stack AG, van Duin AC, Logan BE. Effect of strong acid functional groups on electrode rise potential in capacitive mixing by double layer expansion. Environ Sci Technol 2014;48(23):14041–8.
[14] Brogioli D. Extracting renewable energy from a salinity difference using a capacitor. Phys Rev Lett 2009;103(5):058501.
[15] Sales BB, Saakes M, Post JW, Buisman CJN, Biesheuvel PM, Hamelers HVM. Direct power production from a water salinity difference in a membrane-modified supercapacitor flow cell. Environ Sci Technol 2010;44(14):5661–5.
[16] Zhu X, Yang W, Hatzell MC, Logan BE. Energy recovery from solutions with different salinities based on swelling and shrinking of hydrogels. Environ Sci Technol 2014;48(12):7157–63.
[17] Fanaian S, Al-Manasir N, Zhu KZ, Kjøniksen AL, Nyström B. Effects of Hofmeister anions on the flocculation behavior of temperature-responsive poly(N-isopropylacrylamide) microgels. Colloid Polym Sci 2012;290(16):1609–16.
[18] Arens L, Weibenfeld F, Klein CO, Schlag K, Wilhelm M. Osmotic engin: translating osmotic pressure into macroscopic mechanical force via poly(-acrylic acid) based hydrogel. Adv Sci 2017;4(9):1700112.
[19] Bui TQ, Cao VD, Do NBD, Christoffersen TE, Wang W, Kjøniksen A-L. Salinity gradient energy from expansion and contraction of poly(allylamine hydrochloride) hydrogels. ACS Appl Mater Interfaces 2018;10(26):22218–25.
[20] Zavahir S, Krupa I, Almaadeed SA, Tkac J, Kasak P. Polyzwitterionic hydrogels in engines based on the anipoyelectrolyte effect and driven by the salinity gradient. Environ Sci Technol 2019;53(15):9260–8.
[21] Bui TQ, Cao VD, Wang W, Kjøniksen A-L. Recovered energy from salinity gradients utilizing various poly(acrylic acid)-based hydrogels. Polymers 2021;13(4):645.
[22] Shen W, Huang H, Pang Y, Su X. Review of the energy saving hydraulic system based on common pressure rail. IEEE Access 2017;5:655–69.
[23] Lin Y, Bao J, Liu H, Li W, Tu L, Zhang D. Review of hydraulic transmission technologies for wave power generation. Renew Sustain Energy Rev 2015;50:194–203.
[24] Ricci P, Lopez J, Santos M, Ruiz-Minguela P, Villate JL, Salcedo F, et al. Control strategies for a wave energy converter connected to a hydraulic power take-off. IET Renew Power Gener 2011;5(3):234–44.
[25] He X, Xiao G, Hu B, Tan L, Tang H, He S, et al. The applications of energy regeneration and conversion technologies based on hydraulic transmission systems: a review. Energy Convers Manag 2020;205:112413.
[26] Xia L, Quan L, Ge L, Hao Y. Energy efficiency analysis of integrated drive and energy recuperation system for hydraulic excavator boom. Energy Convers Manag 2018;156:680–7.
[27] He X, Liu H, He S, Hu B, Xiao G. Research on the energy efficiency of energy regeneration systems for a battery-powered hydrostatic vehicle. Energy 2019;178:400–18.
[28] Ehsani M, Gao Y, Emadi A. Modern electric, hybrid electric, and fuel cell vehicles: fundamentals, theory, and design. CRC Press 2009.
[29] Li C, Tse PW. Fabrication and testing of an energy-harvesting hydraulic damper. Smart Mater Struct 2013;22.
[30] Zhang Y, Zhang X, Zhan M, Guo K, Zhao F, Liu Z. Study on a novel hydraulic pumping regenerative suspension for vehicles. J Franklin Inst 2015;352:485–99.
[31] Hamer WJ, Wu Y-C. Osmotic coefficients and mean activity coefficients of uni-univalent electrolytes in water at 25 oC. J Phys Chem Ref Data 1972;1(4):1047–99.
[32] Wilczek-Vera G, Rodil E, Vera JH. Towards accurate values of individual ion activities: additional data for NaCl, NaBr and KCl, and new data for NH4Cl. Fluid Phase Equil 2006;241(1):59–69.
[33] Khoshkbarchi MK, Vera JH. Measurement and correlation of ion activity in aqueous single electrolyte solutions. AIChE J 1996;42(1):249–58.